Comparison of Neutral point clamped converter and five level diode clamped converter for identifying safe operating limits of grid connected wind turbine

Mrs. E Sreeshobha[1], MD. Jaber Imaduddin Ahmed[2]

[1]Assistant Professor, UCE, Osmania University, Hyderabad

[2]PG Scholar ME PES (EEE), UCE, Osmania University, Hyderabad

Abstract:-

In this project Wind energy conversion systems (WECS) include a variety of non-linear power electronic devices which have a significant contribution towards harmonic emissions. Harmonic emissions are threat for electrical power quality. Hence, harmonic analysis and mitigation has become an integral part of WECS. Multilevel inverters have been widely used for harmonic mitigation with the added benefits of low switching stress and high voltage capability. In this project compare the Neutral point clamped inverter and Diode clamped multi-level inverters are developed with PI-control and PWM techniques for control the harmonics. The validity of the proposed topology has been verified by simulation.

Index terms: Permanent Magnet Synchronous Generator (PMSG), Neutral point clamped inverter, Diode clamped multi level inverter, PWM, PI controller

I. INTRODUCTION

The share of distributed generation (DG) in various countries' contemporary electric power systems is steadily rising. A large portion of distributed generation (DG), which has historically been used for energy conversion but is now being employed for grid support functions [1], comes from wind power, a renewable energy source. Different types of power converters have been suggested for the integration of renewable energy sources into the distribution system [2]. Because they can transfer high power using mature power semiconductor technology with lower voltage stress on semiconductor switches, better waveforms, and a lower cost, multilevel inverters have long been the preferred choice for high-power applications in industrial drives and, more recently, in wind power generation systems.

The main problems with wind generation systems generally are fluctuations in available power due to changing wind speeds, as well as variations in the frequency and voltage of the generator output when synchronous generators are utilized with variable speed wind turbines (VSWT). To overcome these difficulties, an AC/DC/AC system is used to decouple the frequency and voltage of the generator from those of the grid. The output of the synchronous generator is rectified to DC first, and a DC-AC power converter that operates with constant voltage and frequency then connects to the grid. A grid side converter that connects with the grid at the right frequency and voltage and a machine side converter that converts AC to DC are both employed in such a configuration. Additionally, it contains all required grid support features. In high-power wind generation systems that include either a single high-power wind generator or a pool of power accessible from a wind farm, the converter's rating should correspond to the highest power transmitted from the wind production system. In this study, a three phase diode bridge rectifier (DBR), which is readily accessible in the required high power ratings, is used as a machine side converter. A grid-side converter is the main problem since it requires regulated switches with high voltage and power ratings. In this investigation, a diode clamped multilevel inverter (DCMLI) served as the grid side converter. In order to inject a current based on the wind turbines maximum output under The DCMLI is utilized as a voltage source inverter (VSI)

in the current control (CC) mode, depending on the wind conditions at the time. Additionally, it offers load correction for local loads at the point of common connection (PCC). The converter must have a higher rating than the generator due to the added duty of providing local load adjustment. Depending on its rating, the DCMLI can partially or fully compensate the load currents so that the source (grid) currents drawn are balanced, pure sinusoidal, and in phase with the PCC voltages. Multi-level inverters come in three distinct topologies, however because the DCMLI only needs one DC supply, it has an advantage over the others in wind turbine applications It explains why a synchronous generator coupled to a three phase diode bridge rectifier only generates one isolated DC source. The modified DCMLI [3] offers the advantage of employing fewer blocking diodes while maintaining the simplicity of the original DCMLI's architecture. However, the common issue of voltage balancing between the capacitors must be addressed in order to ensure the steady operation of a DCMLI, and two solutions have been suggested [4], [5].

Both of these options—external balancing circuits and particular PWM techniques—have advantages and drawbacks, such as increased control complexity and difficulty of control for specific operating conditions for the former and for specific operating conditions for the latter. Several methods are currently used to control inverters. Hysteresis management of power converters has gained a lot of traction due to its advantageous dynamic characteristics and simplicity of implementation for two-level inverters [6]. This technology has problems with varied and uneven switching frequencies for different switches in a VSI, though. This leads to uneven charging/discharging and unbalancing of the dc link capacitors when utilized for multilevel converter control [7]. The ramp-comparison modulation technique of two level inverters offers tremendous promise for the management of multilayer inverters [8] to overcome the issue of variable and uneven switching frequencies due to its virtue of a consistent switching frequency determined by the triangular carrier frequency.

In this study, a control approach for the modified topology DCMLI with a smaller number of diodes is presented for achieving both local load correction and the grid interface of wind power systems. A novel fixed frequency current control method based on level-shifted multi carrier PWM modulation is suggested to achieve the necessary control objectives with equal and uniform switching frequency operation. A need has been developed to guarantee continuous frequency functioning at all times for the proposed modulation approach. The inverter power output to the grid is adjusted to match the available power at the wind turbine in order to evacuate the power available from the wind turbine in accordance with the wind conditions.

If, as illustrated in the curve in Fig. 1, the reliability and corresponding cost of a power semiconductor for a wind power converter are related, the "just-right" device cost/ratings can be computed based on the particular dependability requirements of the mission profile. Using this reliability-cost model and the "reliability-oriented" design process, it is possible to build the wind power converter more precisely and affordably while still adhering to the goal reliability requirements. The reliability-cost performance profiles can also be utilized to more meaningfully unite and evaluate various converter systems, as demonstrated in Fig. 2.
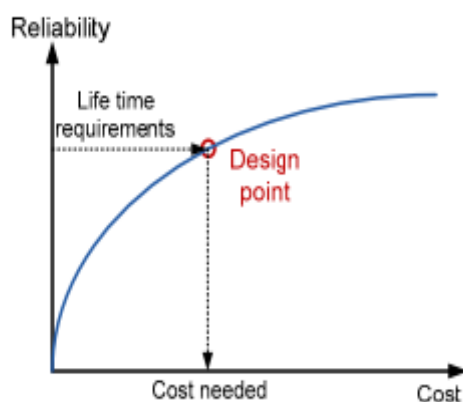

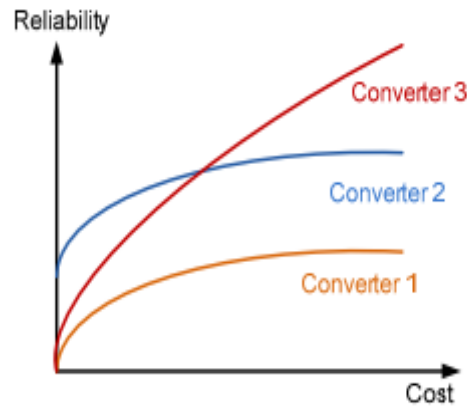Fig. 1 A converter's reliability-cost profile

Fig. 2 Comparison of the reliability-cost profiles of several converter solutions

For instance, converter solutions for a specific mission profile with various topologies, voltage ratings, switching frequency, and so forth. This has led to the development of a new reliability-cost evaluation criteria for wind power.

The diagram below shows the fundamental design of a PMSG wind turbine. 5 The wind turbine produces torque using wind energy. The generator shaft transmits the torque to the generator rotor. Whether the mechanical system accelerates, decelerates, or maintains a constant speed depends on the difference between the mechanical torque produced by the wind turbine and the electrical torque produced by the generator. The generator is connected to a three-phase inverter, which corrects the current and charges a DC-link capacitor. The DC-link feeds a second three-phase inverter, which is connected to the grid through a transformer. The control system accepts wind speed, pitch angle, rotor RPM, and inverter output for comparison with grid-side data. In order to create the correct signal for controlling these components, a digital signal processing system is used to solve this challenge. Connecting to the electric grid and supplying it with power is the main goal.

II. SPEED AND POWER RELATIONS OF A WIND TURBINE

A. Modeling of Wind Turbines

To examine the efficiency of energy conversion in wind energy conversion systems, it is necessary to first calculate the amount of energy that can be stored in the wind. In actuality, wind energy can be thought of as the kinetic energy of numerous air particles having a total mass of m and a wind speed of VW. Assuming that every air particle is travelling in the same direction and at the same speed before it reaches the wind turbine's rotor blades, the potential accessible kinetic energy contained in the wind can be expressed as follows:

$$E = \frac{1}{2} m V_w^2 \qquad (1)$$

Where

E stands for the kinetic energy of moving air particles, m for their total mass, and VW for their velocity (wind speed).

$$P_M = 0.5 \times \rho \times C_P(\lambda, \beta) \times A \times V_{Wind}^3 \qquad (2)$$

Where

Pm is the mechanical output power (W) of the turbine, A denotes the swept area (m2), Vwind denotes the wind speed (m/s), and Cp denotes the power coefficient of the turbine. The tip-to-tip-to-tip-to-tip-to Cp, or power coefficient, is defined as the ratio of the rotor blades tip speed to the wind speed.

$$C_P(\lambda,\beta) = C_1\left(\frac{C_2}{\lambda_1} - C_3 \times \beta - C_4\right) \times e^{\frac{-c_5}{\lambda i}} + C_6 \times \lambda$$

(3)

$$\lambda = \frac{R \times W_M}{V_{WIND}}$$

Where

C1 = 0.5176,

C2 = 116,

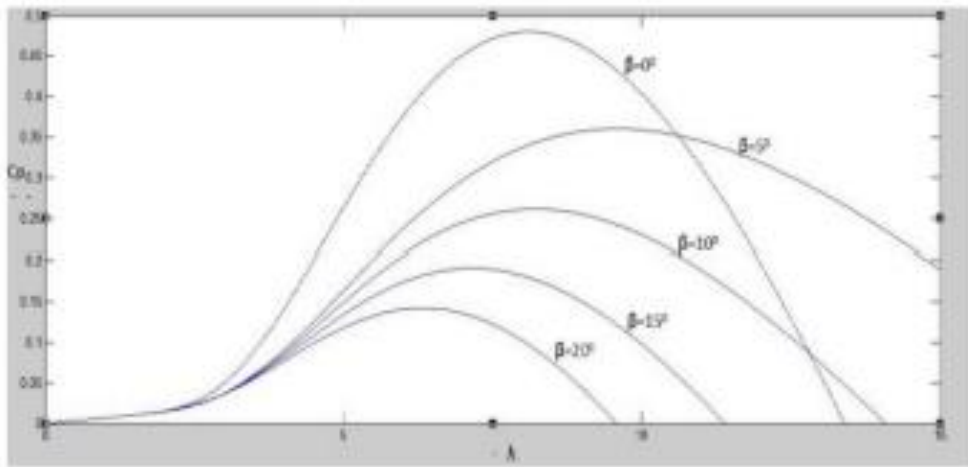C3 = 0.4,

C4 = 5,

C5 = 21, and C6 = 0.0068.

Fig. 3. Curve of Cp Vs Tip Speed Ratio

Figure 3 displays the power coefficient in respect to the tip speed ratio. The largest power coefficient value for = 8 and = 00 is 0.48, according to the expression Cp max = 0.48. The ideal position, where the turbine harnesses the greatest wind energy, is produced by this value of opt.
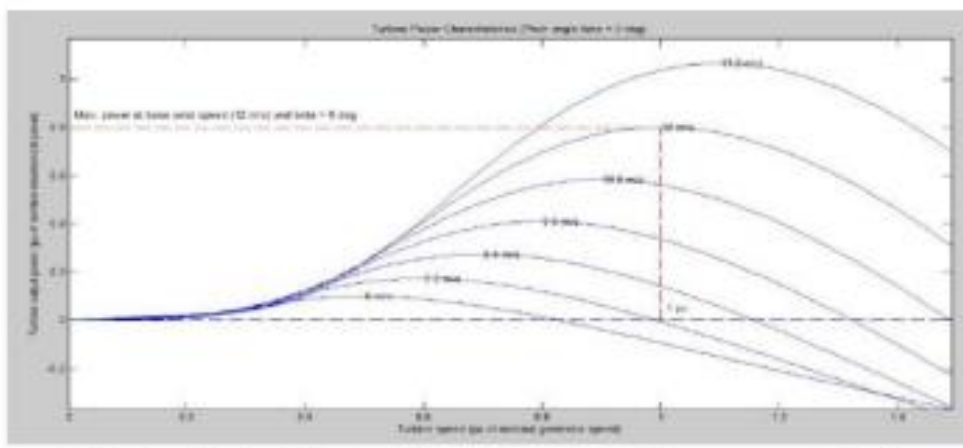

Figure 4: Electricity Properties of Wind Turbines

Figure 4 displays the wind turbine power characteristics calculated for various values of the wind tangential speed. It appears that maximum power (active) is generated at optimum wind speeds as opposed to high wind

speeds. The wind turbine does not operate when the wind speed is below the minimum because the amount of wind energy acquired is insufficient to pay for the losses and operating expenses.

B Modeling of the drive train

This part converts the mechanical torque and machine speed.

$$T_{aero} = g_r \times T_m \qquad (4)$$

$$\Omega_m = g_r \times \Omega \qquad (5)$$

$$J \times \frac{d\Omega}{dt} = T_m - T_e \times f \times \Omega_m \qquad (6)$$

Where

J stands for the mechanical inertia of the wind turbine and generator, Taero stands for the aerodynamic torque,

Te stands for the electromagnetic torque, and f stands for the friction coefficient.

C Modeling of PMSG

The following equations are used to model electrical equipment of the PMSG type. They are represented by the d-q reference frame.

$$V_d = R_s i_d + L_d \frac{dt_d}{dt} - w_e L_q i_q \qquad (7)$$

$$V_q = R_s i_q + L_q \frac{dt_q}{dt} - w_e L_q i_q + w_e \emptyset_e \qquad (8)$$

Where Rs is the stator resistance (ohms), Vd and Vq are the d and q components of the stator voltages (V), id and iq are the d and q components of the stator currents (A), Ld and Lq are the machine inductances (H), and is the magnetic flux (wb).

The electrical torque is calculated using the formula below:

$$T_e = \frac{2}{3} P\{\emptyset_m i_q + (L_d - L_q)i_d i_q\} \qquad (9)$$

$$T_m - T_e = B\omega_r + J\frac{d\omega_r}{dt} \qquad (10)$$

J stands for rotor inertia (kgm2), B for rotor friction (kgm2/s), and ris for rotor speed (rad/s). Tm is the symbol for the mechanical torque generated by wind (Nm). The machine dynamics can be streamlined by presuming (Ld = Lq = 0).
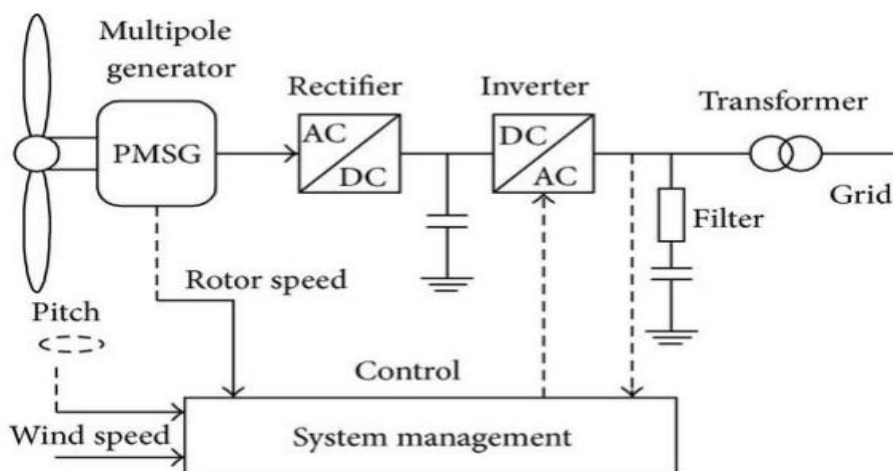

Fig 5 Block schematic of the grid including the wind turbine and the control scheme

III.MULTI-LEVEL INVERTER WITH DIODE CLAMPING

The most common multilevel design is the diode clamped inverter, which uses a diode as a clamping device to limit the dc bus voltage and produce steps in the output voltage. This inverter's fundamental idea is to use diodes to reduce the voltage stress on the power equipment.

Without the necessity for exact voltage matching, the neutral-point clamped (NPC) inverter, sometimes referred to as a diode-clamped inverter, essentially doubles the device voltage level [9]. A five-level diode-clamped converter with four capacitors on the dc bus is shown in Figure 6. (C1, C2, C2, and C4). According to [10]–[12], the voltage across each capacitor for the dc-bus voltage is +Vd2, +Vd1, -Vd1, and -Vd2. If the neutral point n is utilised as the output phase voltage reference point, then there are five switch combinations to synthesise five level voltages across a and n.

1. To get a voltage level Van = Vd1 + Vd2, turn on all upper switches S1–S4.

2. To get a voltage level Van = Vd1, turn on one lower switch S1' and three upper switches S2-S4.

3. Switch on two lower switches S1' and S2', two higher switches S3 and S4, and two switches with a voltage of Van = 0.

4. To get a voltage level Van = -Vd1, activate one higher switch S4 and three lower switches S1' - S3'.

5. For voltage level Van = - Vd1-Vd2, turn on all lower switches S1' through S4'.

As a result, the output waveform's time periods are determined by the transistor switching order, while the voltage levels of the capacitors control the staircase's voltage levels.
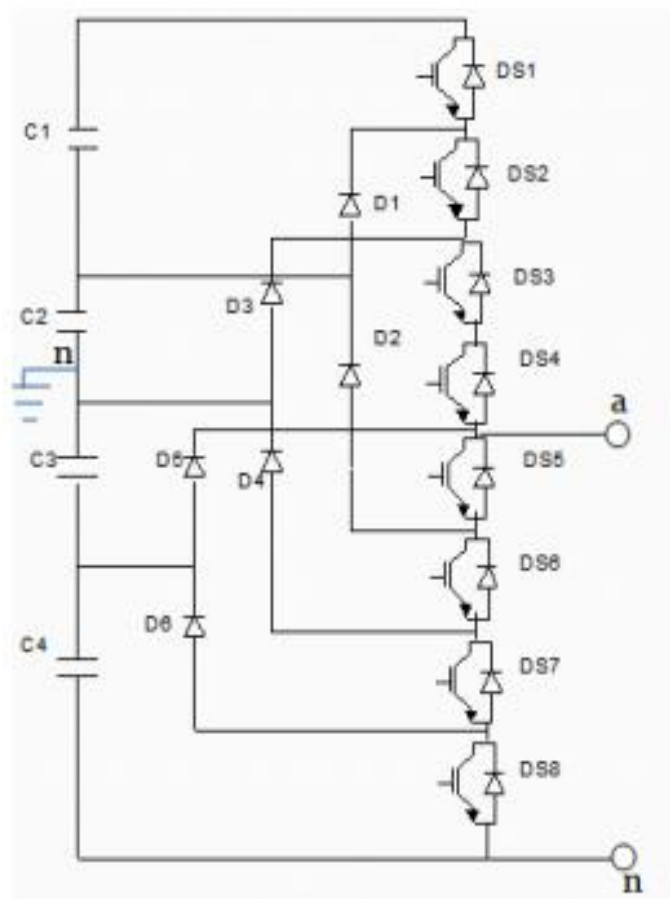

Fig.6. Five-Level Diode Clamped Inverter

In a multilayer inverter, (n-1) determines the number of DC bus capacitors, (n-1) determines the number of switches, (n-1) determines the voltage source, and (n-1) determines the clamping diode (n-2). An inverter's level count is indicated by the letter "n." "Fig. 6" shows a five-level inverter.

Table 1

Clamped five-level inverter with switching states diode

Switching States	Output Voltage	Ds1	Ds2	Ds3	Ds4	Ds5	Ds6	Ds7	Ds8
+2	Vdc/2	1	1	1	1	0	0	0	0
+1	Vdc/4	0	1	1	1	1	0	0	0
0	0	0	0	1	1	1	1	0	0
-1	-Vdc/4	0	0	0	1	1	1	01	0
-2	-Vdc/2	0	0	0	0	1	1		1

In this circuit, the DC bus voltage is separated into three levels as illustrated. A five-level diode-clamped converter is produced by the DC bus, which comprises of four capacitors C1, C2, C3, and C4. The voltage across each capacitor is Vdc/4, and each device's voltage stress is limited to one capacitor voltage level Vdc/4 using clamping diodes. Switches S1 through S4 should be turned on for voltage levels Van=Vdc/2. For a voltage level Van=Vdc/4, turn on three higher switches (S2-S4) and one lower switch (S5). For voltage level Van=0, turn on two top switches S3 and S4, and two bottom switches S5 and S6. For voltage levels Van= -Vdc/4, turn on one upper switch S4 and three lower switches S5-S7. All lower switches should be turned on the S5-S8 NPC inverter, which is frequently used in modern industrial drives, traction, and FACT systems, for voltage levels Van=-Vdc/2. based on the idea that power devices' voltage stress can be reduced by using diodes The output phase voltage can be at any voltage level by selecting any one of the nodes.

A. The three-level inverter circuit layout with the neutral point clamped

The NPCI topology in Figure 7 has three voltage levels for line-to-neutral waveforms and five voltage levels for line-to-line waveforms.

Neutral point clamped (NPC) inverters are a popular multilayer inverter architecture in high-power applications. A few hundred watts too many megawatts of power can be handled by this kind of converter. Neutral-point-clamped (NPC) module: Each leg has four power switches connected in a sequential order. The voltage provided to the power switch is half that of a two-level converter. The NPC topology can function at voltages greater than the voltage rating of a single power device. The top and bottom rows of components, S1u, SIv, SIw and S4u, S4v, S4w, respectively, are connected to the DC bus input, and the phase outputs form the hub of a series connection of four IGBTs. The centre of the DC bus, which is connected to a pair of series-connected diodes in each phase, is represented by a ground sign.
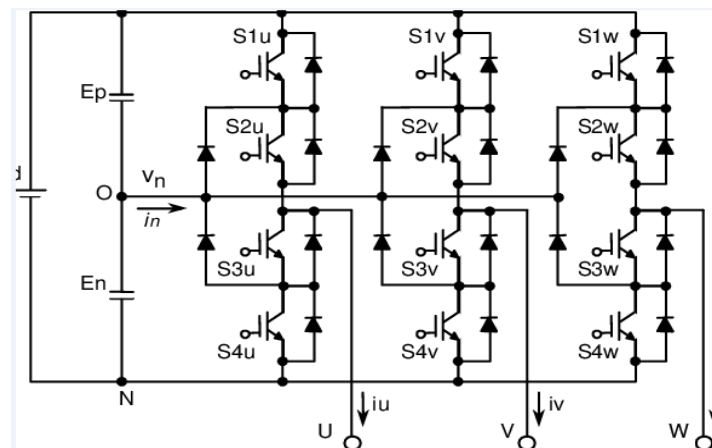

Fig. 7. Circuit topology for a three-level inverter with a clamped neutral point

These six clamping diodes attached to the neutral bus regulate the voltage between the four IGBTs in each phase leg. In a conventional inverter, the switches must preserve the entire voltage drop between the positive and negative DC buses. The voltage drop (stress) across each NPCI switch, however, is equal to half the voltage between the positive and negative bus since the switches on either side of the neutral bus are connected in series and there is a true neutral point. The IGBT gate and emitter terminals must be referenced to each IGBT's unique gate signal. The internal "body diode" that is seen between each IGBT's collector and emitter is a component of the device's design. The DC bus has a positive, negative, and neutral connection thanks to large low frequency filter capacitors and smaller high frequency filter capacitors. The bus structure is covered in more detail in the physical system section.

Table 2

Grid side NPC switching states

S2a	S1a	S2a*	S1a*	S2b	S1b	S2b*	S1b*	Va0	Vb0	Vab
0	0	1	1	1	1	0	0	-Vdc/2	Vdc/2	-Vdc
0	0	1	1	0	1	1	0	-Vdc/2	0	-Vdc/2
1	1	0	0	1	1	0	0	-Vdc/2	Vdc/2	0
0	0	1	1	0	0	1	1	-Vdc/2	-Vdc/2	0
0	1	1	0	0	0	1	1	0	-Vdc/2	Vdc/2
1	1	0	0	0	0	1	1	Vdc/2	-Vdc/2	Vdc

Instead of the 2-level switching seen in conventional 3-phase inverters, 3-level switching is utilised in this NPCI architecture. The three levels stand in for the positive, negative, and neutral buses. The leg A of Figure 7's figure output A is linked to the positive bus by turning on switches S1u and S2u. Switches S3u and S4u are used to connect the phase A output to the negative bus, and S2u and S3 are used to connect the phase A output to the neutral bus. Phase shifted results compared to phase A are produced by the final two phases, which operate similarly to phase A.

B. Sinusoidal Pulse Width Modulation (SPWM)

Similar to multiple pulse modulations, this modulation method employs several pulses every half cycle (MPM). All MPM pulses have the same pulse width. However, with SPWM, the pulse in a cycle is a sinusoidal function of the pulse width. When using Sinusoidal Pulse Width Modulation, many triangular carrier signals are compared to a single modulating Sinusoidal signal.

A five-level inverter needs four triangular carriers, as seen in Figure 8. It is necessary to have (m-1) carrier signals when utilizing an m-level inverter. The carrier signals' frequency fc and peak-to-peak amplitude Ac will be the same. A high-frequency carrier signal and a sinusoidal signal with the necessary frequency are compared to one another at each given moment. The signal is transferred to the appropriate semi-conductor switch in the corresponding legs if the modulating signal in this comparison is larger than the triangle carrier signal.

C Controller in PI

PID controllers relate the error to the actuation signal using a proportional (P), integral (I), or derivative (D) relationship. The controller is a crucial component of the wind turbine system since it has a significant impact on crucial wind turbine performance factors such power quality, noise level, fatigue, and excessive loads. The controller is typically the first part to be updated when a wind turbine's performance is subpar.
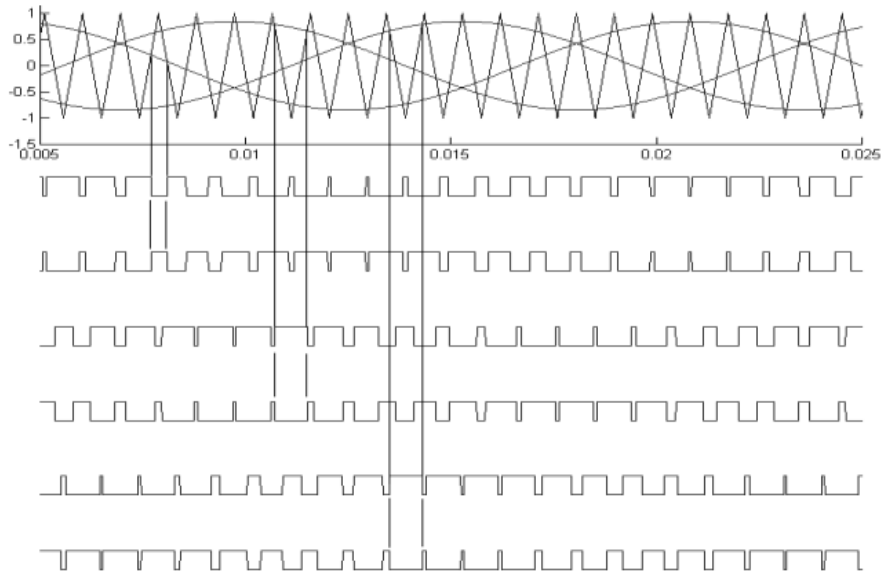
Fig. 8: Creating pulses in connection to fundamental waveforms

There are two distinct zones for the operation of wind turbines, each with a unique set of objectives and command systems. Maximizing power generation is the controller's objective in the partial load sector, which is located below the rated wind speed. In this area, a generator torque controller is used to adjust the rotational speed in order to attain the ideal tip speed ratio. In the full load region, which is over the rated wind speed, the controller's responsibility is to control rotational speed and power. Most frequently, a PI controller is used to control this area. A P.I. Controller is a type of feedback control loop that figures out an error signal by contrasting system outputs. Gain scheduling is necessary to adapt the controller's gains to the continually changing aerodynamic gains, though, as a result of the wind turbine's nonlinearity and the fact that the aerodynamic gains change with wind speed. There is systematic controller tuning methods available for at least some of the controller parameters, despite the fact that trial and error processes are frequently employed to tune wind turbine controllers.

$$\Delta m = K_p \left(\frac{\tau d}{\tau_s} + 1 \right) \Delta e \quad \text{---Proportional term}$$

$$\Delta m = \frac{K_p}{\tau_i} \int e \, dt \quad \text{---- Integral term}$$

IV. SIMULATION DISCUSSION

A PMSG can be connected to the grid effectively using a back-to-back converter. Control systems can achieve unity power factor in the grid connection. Early control systems sought to maximize output from a wind turbine given the current wind conditions. This process is known as peak power extraction, often referred to as maximum power point tracking.

The wind turbine and PMSG are modelled using MATLAB, and its parameters are calculated. Reduce the amount of harmonic and nonlinear loads produced by power electronic converters. The 3L neutral point clamped inverter and the Diode clamped multilayer inverter for the wind energy system were developed using Simulink. The performance metrics for the suggested converter are assessed in the table below, and the results are confirmed.

Table 3

Details the 10 MW 3L-NPC wind power converter's specifications.

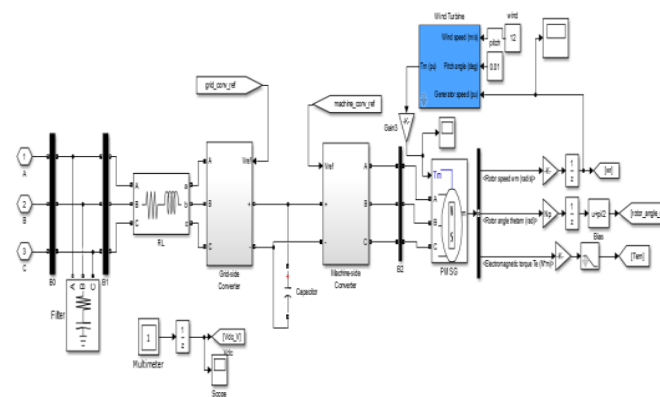| Rated output power Po	10MW
DC bus voltage Vdc	5.6 kv DC
Rated primary side voltage V_g	3.3kv rms
Rated line-line grid voltage V_g	20kvrms
Rated Phase current I_{phase}	1750A rms
Carrier frequency f_c	800Hz
Filter inductance	1.13 mH (0.2 p.u.)
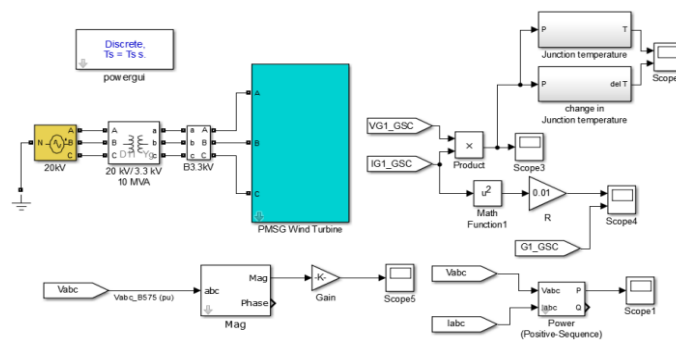
Fig. 9 modeling a wind turbine with MATLAB Simulink

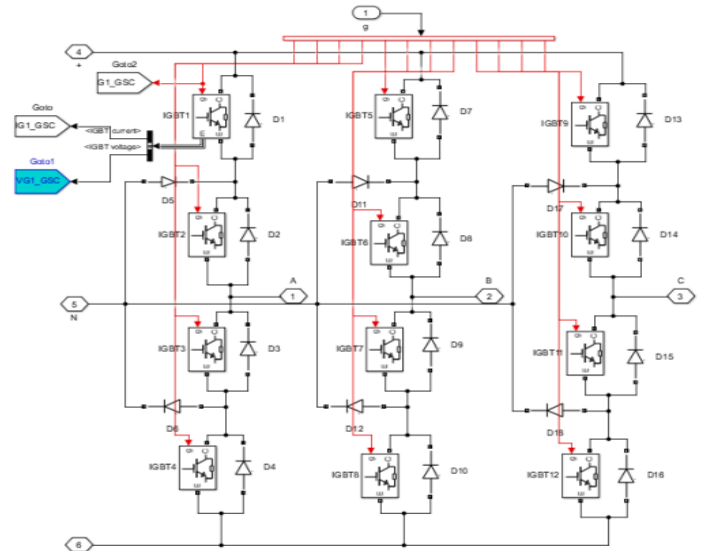Fig. 10 Model for grid connectivity with converters arranged back to back

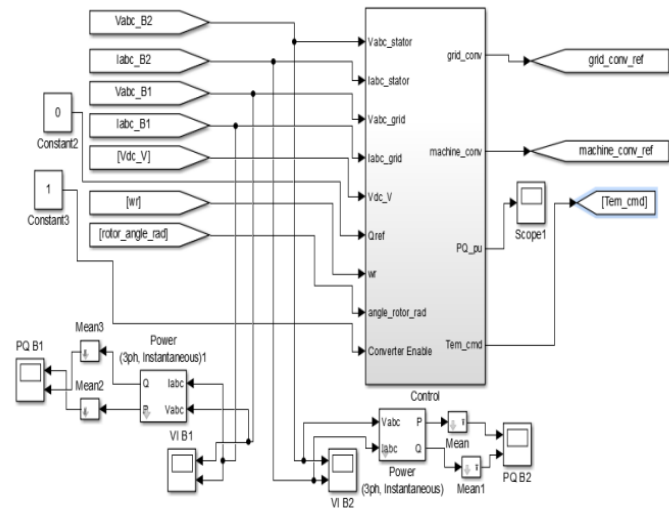Fig. 11 3-level converter with a clamped neutral point
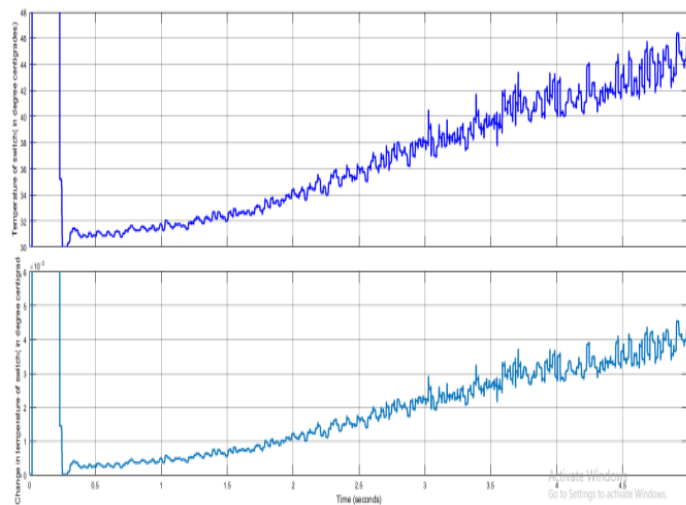

Fig. 12 Model control strategy

Fig. 13: Temperature and variation in temperature (in degree centigrade) Period in v/s (in sec)

For 4.6MW power output, IGBT switches heat up to 46°C, and the temperature variation between two instants of time is negligible in comparison to the prior instant.
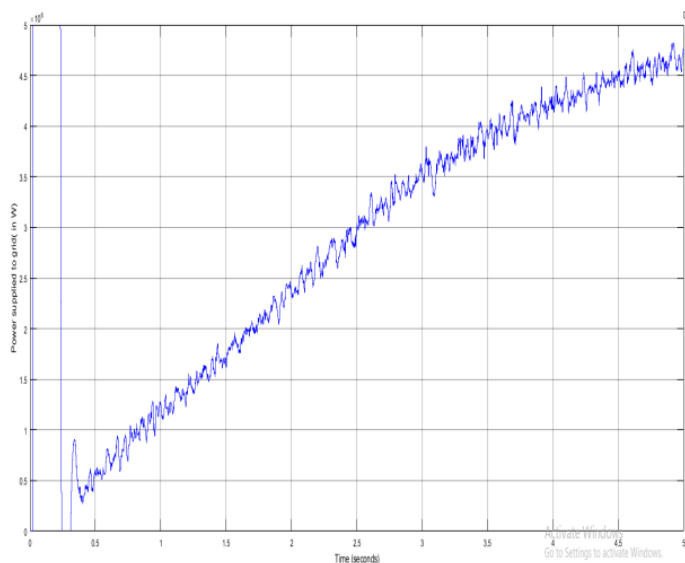

Fig. 14: Time and grid power supply (in W) (in sec)

The power delivered to the grid is around 4.9 MW at a speed of 18 m/s (44 mph); below this speed, the system is unable to produce any power; as a result, this speed is the bare minimum needed for the PMSG turbine to produce the most power.

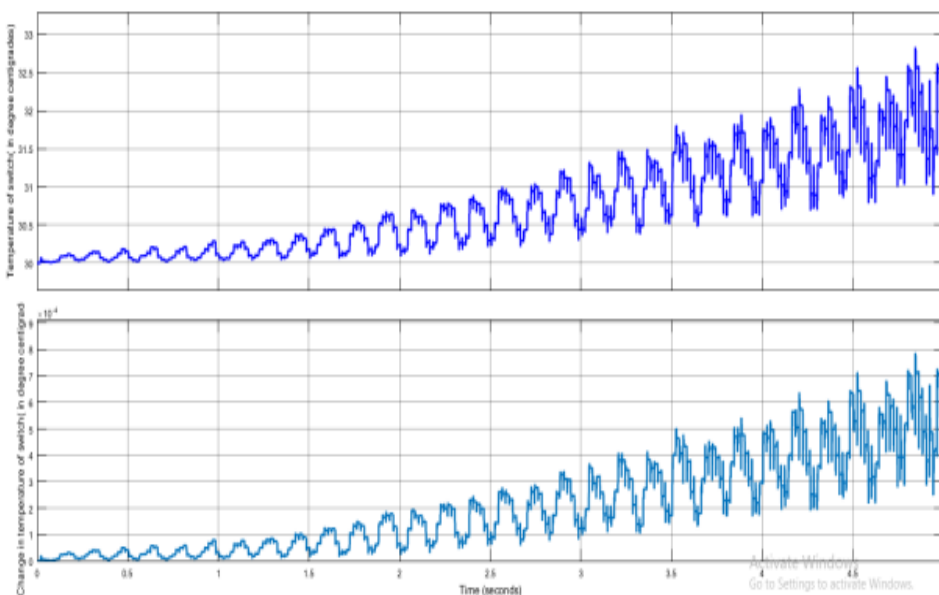**For five level diode clamped converter**

Fig. 15: Temperature and variation in temperature (in degree centigrade) Period in v/s (in sec)

For 4.9MW power output, IGBT switches heat up to 45°C, and the temperature variation between two instants of time is negligible in comparison to the prior instant.
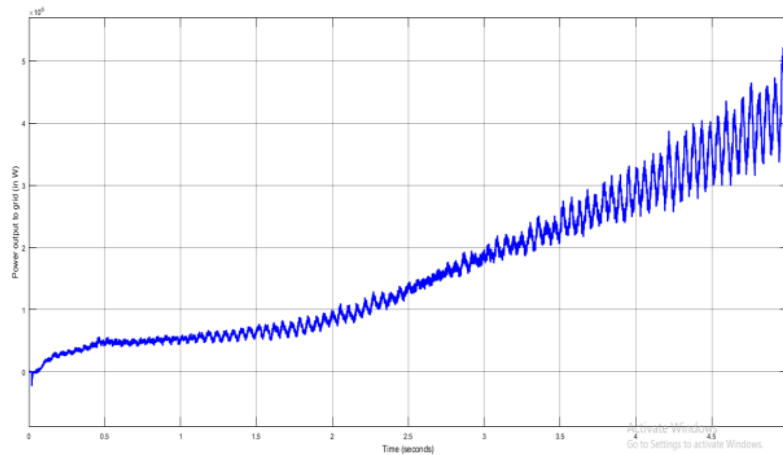
Fig. 16: Time and grid power supply (in W) (in sec)

Figs. 13 to 16 display the temperature and wind energy required to power a grid with regulated AC voltage. The diode clamped multilayer inverter has a greater temperature and produces more power than the NPCI converter. In the end, a finding shows that DCMI has a low THD value.

Table 2

For a 5 level diode clamped converter

Wind speed	Power loss of switch (W)	Temperature of switch (in degree centigrade)	Power supplied to grid (in MW)	THD
12	4000	31	4.3	0
14	4200	32	4.4	0
16	4300	32	4.6	0
18	4400	32.5	4.7	0

Table-3

For Neutral Point Clamped Converter (NPCC)

Wind speed	Power loss of switch (W)	Temperature of switch (in degree centigrade)	Power supplied to grid (in MW)	THD
12	8000	42	4.6	7.68
14	8200	43	4.8	7.68
16	8300	44	4.7	7.65
18	8300	45	4.8	7.63

CONCLUSION

A wind turbine may produce a maximum power of 4-6MW in a system with a speed range of 12m/s to 18m/s when using back-to-back converters with neutral point clamped & Diode clamped multilevel inverter design. Grid-side converters and machine converters' output voltage and power are evaluated. Switching losses and temperature levels in converter devices are simulated using MATLAB. The results will be used to build a heat sink for the converter and determine the system's safe operating wind speeds. A diode clamped multi-level inverter uses diodes as a clamping device to limit the dc bus voltage in order to achieve low THD values. Comparing the results above, DCML performs better.

REFERENCES

1) K. Ma, F. Blaabjerg, D. Xu, "Power Devices Loading in Multilevel Converters for 10 MW Wind Turbines," in Proc. of ISIE 2011, pp. 340-346, June 2011.

2) K. Ma, F. Blaabjerg, "Multilevel Converters for 10 MW Wind Turbines," in Proc. of EPE 2011, pp. 1-10, 2011.

3) K. Ma, F. Blaabjerg, M. Liserre, "Thermal analysis of multilevel grid side converters for 10 MW wind turbines under Low Voltage Ride Through," in Proc. of ECCE 2011, pp. 2117 - 2124, Sep 2011.

4) F. Blaabjerg, M. Liserre, K. Ma, "Power Electronics Converters for Wind Turbine Systems," IEEE Trans. on Industrial Applications, vol. 48, no. 2, pp. 708- 719, 2012.

5) F. Blaabjerg, U. Jaeger, S. Munk-Nielsen and J. Pedersen, "Power Losses in PWM-VSI Inverter Using NPT or PT IGBT Devices," IEEE Trans. on Power Electronics, vol. 10, no. 3, pp. 358–367, May 1995.

6) W. Lixiang, J. McGuire,R.A. Lukaszewski, "Analysis of PWM Frequency Control to Improve the Lifetime of PWM Inverter," IEEE Trans. on Industrial Applications, vol. 47, no. 2, pp. 922-929, 2011.

7) Infineon Application Note: Thermal Resistance Theory and Practice, Jan 2000.

8) Website of ABB semiconductors Available on :http://www.abb.com/product/us/9AAC910029.aspx

9) Dell Aquila A., Monopoli V.G., and Liserrre M., "Control of H-bridge Based Multilevel converters," in IEEE Trans. Power Electron., Oct.2002, pp. 766–771.

10) A. Muthuramalingam, M. Balaji and S. Himavathi, "Selective Harmonic Elimination Modulation Method for Multilevel Inverters," India International Conference on Power Electronics, 2006.

11) S. Khomfoi, L. M. Tolbert, "Multilevel Power Converters," Chapter 17, Power Electronics Handbook, 2nd Edition, Elsevier, ISBN 978-0-12-088479-7, pp. 451-482, 2007.

12) J. N. Chiasson, L. M. Tolbert, K. J. McKenzie, Z. Du, "A complete solution to the harmonic elimination problem," IEEE Transactions on Power Electronics, vol. 19, no. 2, pp. 491-499, 2004.

13) I. Erlich, F. Shewarega, C. Feltes, F. Koch, and J. Fortmann, "Offshore wind power generation technologies," Proceedings of the IEEE, vol 101, no 4, pp 891-905, April 2013.

14) H. Polinder, J. A. Ferreira, B. B. Jense, A. B. Abrahamsen, K. Atallah, and R. McMahon, "Trends in wind turbine generator systems," IEEE Journal of Emerging and Selected Topics in Power Electronics, vol 1, no 3, pp 174-185, September 2013.

15) F. Blaabjerg and K. Ma, "Future on power electronics for wind turbine systems," IEEE Journal of Emerging and Selected Topics in Power Electronics, vol 1, no 3, pp 139-152, September 2013

16) D. Zhou, F. Blaabjerg, M. Lau, and M. Tonnes, "Thermal analysis of multi-MW two-level wind power converter," IECON 2012 - 38th Annual Conference on IEEE Industrial Electronics Society, 2012.

17) L. Clotea and A. Forcos, "Power losses evaluation of two and three-level NPC inverters considering drive applications," Optimization of Electrical and Electronic Equipment (OPTIM), 2012 13th International Conference, 2012

18) J. Li, A. Huang, S. Bhattacharya, and W. Jing, "Application of active NPC converter on generator side for MW direct-driven wind turbine," Applied Power Electronics Conference and Exposition (APEC), 2010 Twenty-Fifth Annual IEEE, pp 1010-1017, 2010.

19) O. Senturk, L. Helle, S. M. Nielsen, R. Teodorescu, and P. Rodriguez, "Power density investigations for the large wind turbines grid-side press-pack IGBT 3L-NPC-VSCs," Energy Conversion Congress and Exposition (ECCE), 2012 IEEE, 2012.

20) X. Jing, J. He, and N. Demerdash, "Application and losses analysis of ANPC converters in doubly-fed induction generator wind energy conversion system," Electric Machines & Drives Conference (IEMDC), 2013 IEEE International, 2013.